Diboson Physics in ATLAS

D. S. Levin*
on behalf of the ATLAS Collaboration

October 28, 2008

*The University of Michigan, Ann Arbor, MI, USA

(received 24 October 2008 ; accepted DDMMYYYY)

Abstract

At the LHC, the diboson states, W^+W^-, ZZ, $W^\pm Z$, $W^\pm\gamma$, and $Z\gamma$ arise primarily through quark-quark interactions and to a lesser extent from gluon-gluon fusion. Diboson production cross-sections are determined in the Standard Model (SM) at tree level by t- and u-channel diagrams and by charged triple-gauge-boson couplings in the s-channel. Possible anomalous triple gauge couplings, reflecting non-SM physics, can increase diboson production. We report on the studies of expected ATLAS measurements of diboson production cross-sections in the leptonic (electron and muon) decay channels of the W and Z bosons. Such potential measurements can probe anomalous triple gauge boson couplings and are sensitive to physics beyond the SM.

ATL-PHYS-PROC-2008-051
29 October 2008

1 Introduction

This paper summarizes studies [1] of Standard Model (SM) dibosons WW, WZ, ZZ, $W\gamma$ and $Z\gamma$ detection sensitivities in ATLAS with final states containing muons, electrons and photons, and associated triple gauge boson couplings (TGC). Many models predict the anomalous couplings of the order of $10^{-3} - 10^{-4}$ [2]. Anomalous couplings yield larger diboson cross-sections, particularly at high transverse momentum, p_T, of the bosons and high transverse mass, M_T, of the dibosons. Experimental limits on anomalous TGC's are obtained by measuring deviations of these distributions from theoretical predictions. This study is based on an initial (early LHC running) ATLAS detector and trigger description.It uses 30 million fully simulated events for a refined understanding of the backgrounds and employs a *Boosted Decision Tree* algorithm [3] (BDT) for a significant enhancement of the detection sensitivity.

Tree-level Feynman diagrams for electroweak diboson production at hadron colliders are shown in Figure 1. The s-channel diagram contains the vector-boson self-interaction vertices of interest. SM cross-sections are available up to next-to-leading-order (NLO) [4], [5], [6] and are shown in Table 1.

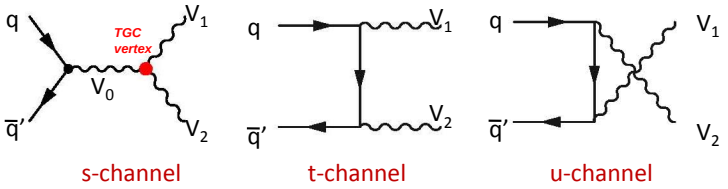

Figure 1: Tree level diagrams of diboson production in hadron colliders. In the SM, charged boson pairs are produced in all diagrams, neutral pairs only in the t-channel and u-channel. The s-channel contains the TGC vertex. $V_i = W, Z$ or γ.

The most general effective Lagrangian, conserving C and P separately, for charged triple gauge boson interactions is [7]:

$$L/g_{WWV} = ig_1^V(W^*_{\mu\nu}W^\mu V^\nu - W_{\mu\nu}W^{*\mu}V^\nu) + i\kappa_V W^*_\mu W_\nu V^{\mu\nu} + i\frac{\lambda_V}{M_W^2}W^*_{\rho\mu}W^\mu_\nu V^{\nu\rho}$$

where V refers to the neutral vector-bosons, Z or γ; $V_{\mu\nu} \equiv \partial_\mu V_\nu - \partial_\nu V_\mu$ (and similarly for W) and the overall coupling constants g_{WWV} are given by $g_{WW\gamma} = -e$, $g_{WWZ} = -e\ cot\theta_W$, with e the positive electron charge and θ_W the weak mixing angle. In the SM $g_1^V = \kappa_V = 1$ and $\lambda_V = 0$. Experimentally we search for anomalous couplings: $\Delta g_1^Z \equiv g_1^Z - 1$, $\Delta\kappa_\gamma \equiv \kappa_\gamma - 1$, $\Delta\kappa_Z \equiv \kappa_Z - 1$, λ_γ, and λ_Z. Electromagnetic gauge invariance requires $g_1^\gamma = 1$ or $\Delta g_1^\gamma = 0$. The final states W^+W^-, $W^\pm Z$, and $W^\pm\gamma$ have different $\sqrt{\hat{s}}$ dependence, where $\sqrt{\hat{s}}$ is the invariant mass of the vector-boson pair. This provides complementary sensitivity to the charged anomalous TGC's [8]. In the SM, neutral boson pairs, ZZ and $Z\gamma$, are produced via the t- and u-channels. While the SM ZZZ and $ZZ\gamma$ TGC's are zero at tree level, anomalous couplings may contribute. For production of on-shell Z bosons pairs only (as in these studies) the most general form of the effective Lagrangian respecting Lorentz and electromagnetic gauge invariance yields neutral, C odd couplings [9], commonly referred to as f_i^V $(i = 4,\ 5)$. CP invariance and parity conservation forbids f_4^V, and f_5^V respectively.

With non-SM coupling, diboson production amplitudes grow with energy, eventually violating tree-level unitarity. This is avoided by scaling the anomalous parameters: $\Delta\kappa(\hat{s}) = \frac{\Delta\kappa_0}{(1+\hat{s}/\Lambda^2)^n}$, where $\Delta\kappa_0$ is the coupling value in the low energy limit, n=2,3 for charged, neutral TGC respectively. Λ is the mass scale where the new phenomenon responsible for the anomalous couplings would be directly observable.

Table 1: Diboson signatures, cross-sections and event selections.

Process ($l = e, \mu$)	selection (leptons and photons are isolated, all $E_T^{jets} > 30GeV$)
$WW \to l^+ \nu\, l^- \nu$ $\sigma_{WW}^{tot} = 113$ pb	2 opposite sign leptons with $p_T > 25$ GeV, $\Delta R(ll) > 0.2$, $E_T^{miss} > 30$ GeV, $\lvert M_z - M_{ll}\rvert > 30$ GeV, $N_{jet} < 2$, Vector Sum(p_T^{lep}, E_T^{miss})< 100 GeV
$WZ \to l^\pm \nu\, l^+ l^-$ $\sigma_{W^+Z}^{tot} = 29$ pb $\sigma_{W^-Z}^{tot} = 18.4pb$	2 opposite sign +1 lepton with $p_T > 25$ GeV, $\Delta R(ll) > 0.2$, vertex:$\Delta Z(ll) < 1$ mm, $\Delta A(ll) < 0.1$ mm, $E_T^{miss} > 30$ GeV, $\lvert M_z - M_{ll}\rvert < 10$ GeV, $40 < M_T < 250$ GeV, $N_{jet} < 2$, Vector Sum(p_T^{lep}, E_T^{miss})< 100 GeV
$ZZ \to l^+ l^- l^+ l^-$ $\sigma_{ZZ}^{tot} = 14.8$ pb	2 pairs of opposite sign leptons with $p_T > 20$ GeV, $\Delta R(ll) = \sqrt{\Delta\Phi_{ll}^2 + \Delta\eta_{ll}^2} > 0.2$, N_{jet}=0, all leptons same vertex
$ZZ \to l^+ l^- \nu\, \nu$ $\sigma_{ZZ}^{tot} = 14.8$ pb	2 opposite sign leptons, E_T^{miss}, $p_T > 20$ GeV, $\Delta R(ll) > 0.2$, $\lvert M_z - M_{ll}\rvert < 10$ GeV, $E_T^{miss} > 50$ GeV, veto 3^{rd} lep, $p_T(ll) > 100$ GeV, N_{jet}=0, $\Delta\Phi(Z, E_T^{miss}) > 35^0$
$Z\gamma \to l^+ l^- \gamma$ $\sigma_{Z\gamma}^{tot} = 219$ pb	2 opposite sign leptons, photon, p_T and $E_T > 20$ GeV, $\Delta R(ll) > 0.2$, $\Delta R(l, photon) > 0.7$, N_{jet}=0, $\lvert M_z - M_{ll}\rvert < 10$ GeV, $\lvert M_z - M_{ll\gamma}\rvert > 30$ GeV
$W\gamma \to l^\pm \nu\, \gamma$ $\sigma_{W\gamma}^{tot} = 451$ pb	1 lepton and photon $p_T > 20$ GeV, $E_T^{miss} > 30$ GeV, $40 < M_T < 250$ GeV, N_{jet}=0, $\Delta R(l, photon) > 0.7$

Table 2: Diboson detection efficiencies and statistical significance for 1 fb^{-1}

Process	Method	$N_{signal}(S)$	$N_{bkg}(B)$	Eff.	Significance
$WW \to l^+\nu\, l^-\nu$	BDT	469 ± 6	92 ± 8	4.9%	23
	cuts	231 ± 4	223 ± 21	2.4%	15
$WZ \to l^\pm\nu\, l^+l^-$	BDT	128 ± 2	16 ± 3	15.2%	18
	cuts	53 ± 2	8 ± 1	6.3%	11.4
$ZZ \to l^+l^-l^+l^-$	cuts	$17 \pm .1$	$1.9 \pm .2$	7.7%	6.8
$ZZ \to l^+l^-\nu\nu$	cuts	$10 \pm .2$	5 ± 2	2.6%	3.2
$Z\gamma \to e^+e^-\gamma$	BDT	367 ± 12	187 ± 19	5.4%	20.3
$Z\gamma \to \mu^+\mu^-\gamma$	BDT	751 ± 23	429 ± 43	11%	27.8
$W\gamma \to e^\pm\nu\gamma$	BDT	1604 ± 65	1180 ± 120	5.7%	> 30
$W\gamma \to \mu^\pm\nu\gamma$	BDT	2166 ± 88	1340 ± 130	7.6%	> 30

2 Event Generation and Analysis

Generation of W^+W^-, $W^\pm Z^0$, Z^0Z^0 final states and leptonic decays are modeled by the MC@NLO (v3.1) [10] generator, interfaced to HERWIG/Jimmy (v6.5) [11] for NLO QCD matrix elements. WW production via gluon-gluon fusion is done by gg2ww (v2.4) [12]. $W^\pm\gamma$ and the $Z^0\gamma$ production is from PYTHIA (v6.4) [13] with leading order QCD matrix elements. Backgrounds from top pairs are simulated by MC@NLO, and from QCD jets associated with the Ws or Zs are produced by PYTHIA. All cross-sections are normalized to NLO, using k-factors determined from the NLO generators. The diboson processes, production cross-sections ($\sigma(V \to leptons)$) and event selections are reported in Table 1.

Studies of diboson events were conducted with a straight-cut analysis based on selections in Table 1 and also using a multi-variate BDT algorithm [3]. In the latter, a cut on the BDT output discriminant was chosen to minimize the cross-section measurement error. The expected signal and background for 1 fb^{-1} luminosity using one or the other method are reported in Table 2.

To determine sensitivity to anomalous TGC's the BHO and BosoMC MC generators [8] [14] for ZZ, WW, $Z\gamma$ and for WZ, γ respectively are used to compute differential cross-sections over a grid of points in the parameter space. Figure 2(a) shows cross-sections for SM and anomalous TGC's. Rather than

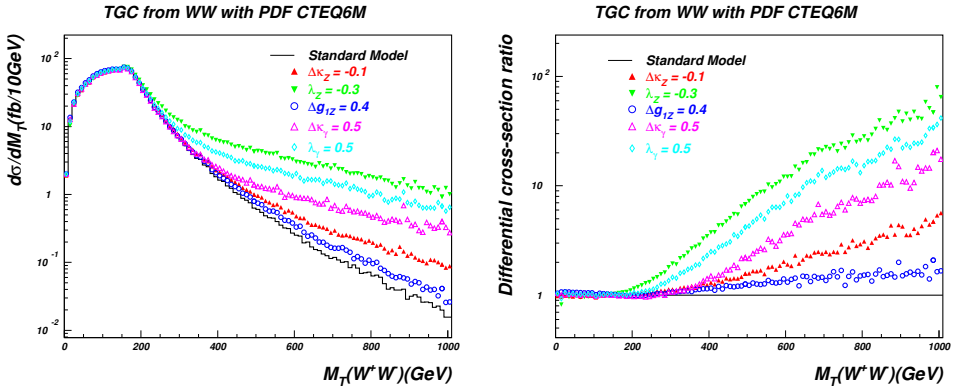

(a) Differential cross-sections with SM and anomalous TGC's

(b) Cross-section ratio (anomalous to SM) vs M_T

Figure 2: Differential cross-Sections vs M_T

Table 3: Charged TGC 95% CL limits, $\Lambda = 2$ TeV

Lumi. fb^{-1}	λ_z WZ	$\Delta\kappa_Z$ WW	Δg_1^Z WZ	$\Delta\kappa_\gamma$ WW	λ_γ $W\gamma$
1	[-0.028,0.024]	[-0.117,0.187]	[-0.021,0.054]	[-0.24,0.25]	[-0.09,0.04]
10	[-0.015,0.013]	[-0.035,0.072]	[-0.011,0.034]	[-0.088,0.089]	[-0.05,0.02]
30	[-0.012,0.008]	[-0.026,0.0048]	[-0.005,0.023]	[-0.056,0.054]	[-0.02,0.01]
D0/CDF best	[-0.13,0.14]	[-0.82,1.27]		[-0.88,0.96]	[-0.2,0.2]

re-run fully simulated events with anomalous couplings, the ratios $d\sigma_{anom}/d\sigma_{SM}$ (Figure 2(b)) are used to re-weight the fully simulated SM events, after standard cuts. Theoretical *reference* distributions of p_T and M_T in coupling parameter space are created. These variables are sensitive to anomalous TGC's, especially at high M_T or p_T as Figure 2(a) shows. To determine experimental sensitivity, pseudo-data are extracted from the SM simulated data as mock observations corresponding to a specified luminosity. Figure 3 shows an 'observed' M_T distribution of W^+W^- pairs for 1 and 30 fb^{-1}. Comparison to a theoretical reference distribution is done with a binned Maximum Log Likelihood (MLL) method. By fitting the MLL to an anomalous TGC parameter, one dimensional 95% CL limits are obtained. Limits on charged anomalous TGC's for 1, 10 and 30 fb^{-1} are reported in Table 3 with Tevatron limits for comparison. One dimensional limits for neutral anomalous TGC's based on $ZZ \to llll$ and $ZZ \to ll\nu\nu$ are in Table 4 with LEP results for comparison. Charged and neutral TGC two dimensional expected limits are available in [1].

Table 4: Neutral TGC 95% CL limits, $\Lambda = 2$ TeV

Luminosity fb^{-1}	f_4^Z	f_5^Z	f_4^γ	f_5^γ
1	[-0.018,0.018]	[-0.018,0.019]	[-0.022,0.022]	[-0.022,0.022]
10	[-0.009,0.009]	[-0.009,0.009]	[-0.01,0.01]	[-0.011,0.01]
30	[-0.006,0.006]	[-0.006,0.007]	[-0.008,0.008]	[-0.008,0.008]
LEP	[-0.3,0.3]	[-0.34,0.38]	[-0.17,0.19]	[-0.32,0.36]

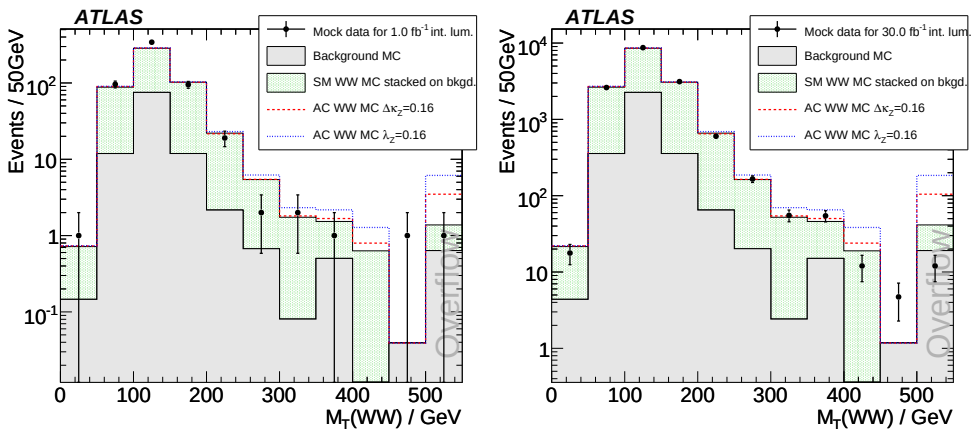

(a) (b)

Figure 3: W^+W^- transverse mass distributions at 1 fb^{-1} (a) and 30 fb^{-1} (b) integrated luminosity. Pseudo-observations (data points) are shown with SM and anomalous coupling (AC) signals combined with background. The last bins are overflow bins.

3 Conclusion

Vector boson self-couplings are a fundamental prediction of the non-Abelian $SU(2)_L \times U(1)_Y$ gauge symmetry theory, thus precise measurements of the couplings are a test of the SM and a probe for new physics. A factor of 7 higher LHC collision energy over the Tevatron enables a higher reach in p_T and M_T. Coupled with cross-sections $10\times$ higher [1], the LHC diboson production rate will be ~ 100 times higher, allowing ATLAS sensitivities to anomalous TGC's to be greatly improved over current limits.

References

[1] ATLAS Collaboration CERN-OPEN-2008-020.- Geneva : CERN, 2008, to appear

[2] J. Ellison and J. Wudka, Annu. Rev. Nucl. Part. Sci. **48**, 33 1998.

[3] A. A. Aguilar-Arevalo et al, Phys. Rev. Lett. **98** 231801 2007.

[4] J.M. Campbell and R.K. Ellis, Phys. Rev. **D60**, 113006 1999.

[5] L. Dixon, Z. Kunszt, A. Signer, Phys. Rev. **D60**, 114037 1999.

[6] J. Ohnemus, Phys. Rev **D47**, 940 1993.

[7] F. Larios, M.A. Perez, G. Tavares-Velasco, J.J. Toscano, Phys Rev **D63**, 113014, 2001.

[8] U. Baur, T Han and J. Ohnemus, Phys. Rev., **D57** 2823 1998.

[9] U. Baur and D. Rainwater, Phys. Rev. **D62**, 2000 113011

[10] S. Frixione and B.R. Webber JHEP 0206 2002, 029

[11] G. Corcella et al, JHEP 0101 (2001) 010 hep-ph/0011363; hep-ph/0210213

[12] T. Binoth, M. Ciccolini, N. Kauer, M. Kraemer, JHEP12, 046, 2006.

[13] T. Sjostrand et al, Comput. Phys. Commun., **135**, 238259, 2001.

[14] M. Dobbs, Ph.D. Thesis, University of Victoria, 2002.